


Effects of interactions on magnetization relaxation dynamics in ferrofluidsAlexey O. Ivanov *Department of Theoretical and Mathematical Physics, Ural Mathematical Center, Institute of Natural Sciences and Mathematics, Ural Federal University, 51 Lenin Avenue, Ekaterinburg 620000, Russia*Philip J. Camp **School of Chemistry, University of Edinburgh, David Brewster Road, Edinburgh EH9 3FJ, Scotland and Department of Theoretical and Mathematical Physics, Institute of Natural Sciences and Mathematics, Ural Federal University, 51 Lenin Avenue, Ekaterinburg 620000, Russia*

(Received 9 July 2020; revised 12 August 2020; accepted 1 September 2020; published 21 September 2020)

The dynamics of magnetization relaxation in ferrofluids are studied with statistical-mechanical theory and Brownian dynamics simulations. The particle dipole moments are initially perfectly aligned, and the magnetization is equal to its saturation value. The magnetization is then allowed to decay under zero-field conditions toward its equilibrium value of zero. The time dependence is predicted by solving the Fokker-Planck equation for the one-particle orientational distribution function. Interactions between particles are included by introducing an effective magnetic field acting on a given particle and arising from all of the other particles. Two different approximations are proposed and tested against simulations: a first-order modified mean-field theory and a modified Weiss model. The theory predicts that the short-time decay is characterized by the Brownian rotation time τ_B , independent of the interaction strength. At times much longer than τ_B , the asymptotic decay time is predicted to grow with increasing interaction strength. These predictions are borne out by the simulations. The modified Weiss model gives the best agreement with simulation, and its range of validity is limited to moderate, but realistic, values of the dipolar coupling constant.

DOI: [10.1103/PhysRevE.102.032610](https://doi.org/10.1103/PhysRevE.102.032610)**I. INTRODUCTION**

Magnetic fluids are useful and inherently interesting types of colloidal suspension. They are composed of small superparamagnetic or large ferromagnetic particles suspended in a simple, nonmagnetic carrier liquid [1]. A key property of such fluids is that the structural and dynamical properties can be switched with the application of magnetic fields. Homogeneous fields align the particle magnetic dipole moments through the Zeeman interaction, and strong fields can lead to extensive chain formation in the field direction. The resulting structural anisotropy has concomitant effects on the magnetic, optical, and viscometric properties of the fluid.

The influence of interparticle interactions on the static magnetic properties of magnetic fluids is well understood. The key properties here are the magnetization curve $M(H)$ and the initial susceptibility $\chi = (dM/dH)_{H=0}$, and these were being studied as long ago as the early 1900s in the context of mean-field theory [2,3]. Modern statistical-mechanical theories of the magnetization curve are much more sophisticated [4–19] and are free of artifacts, such as the prediction of a spontaneous transition to a long-range-ordered ferromagnetic liquid state at low temperature and/or with strong interparticle interactions.

The dynamic magnetic response has also received a lot of attention, and in particular, the initial susceptibility $\chi(\omega)$ of

a magnetic fluid to a weak ac magnetic field with angular frequency ω . Part of the interest in $\chi(\omega)$ is that its imaginary (or out-of-phase) part controls the dissipation of heat [20], and this mechanism can be used in medicine for hyperthermia treatments [21,22]. There are two fundamental mechanisms for the reorientation of a particle in a magnetic fluid [1,23–27]: Néel relaxation in a superparamagnetic particle involves the rotation of the dipole moment within the particle-fixed frame, usually defined by the crystal axes of the constituent magnetic grain, and Brownian rotation of a superparamagnetic or ferromagnetic particle involves the reorientation of the particle as a whole. The latter is strongly influenced by the viscosity of the carrier liquid and the interactions between the particles. The dynamics of magnetic relaxation have been the subject of several experimental [28–37] and simulation [38–46] studies. Theoretically, the influence of the interactions on the so-called dynamic (or frequency-dependent) initial magnetic susceptibility has been evaluated within various approaches [41,42,47–54]. Predictions from modified mean-field approaches (described below) have been tested critically against experimental [35,36] and simulation results [40–42].

The fluctuation-dissipation theorem links the decay of equilibrium thermal fluctuations in the magnetization with the linear response of the magnetization to small changes in the magnetic field. Specifically, the frequency spectrum of the magnetization autocorrelation function $\langle \delta \mathbf{M}(t) \cdot \delta \mathbf{M}(0) \rangle$, where $\delta \mathbf{M}(t) = \mathbf{M}(t) - \langle \mathbf{M} \rangle$, is linked to the dynamic magnetic susceptibility, and this relation has been exploited in equilibrium dynamical simulations [40–42].

*Corresponding author: philip.camp@ed.ac.uk

The subject of this work is the nonequilibrium relaxation of the magnetization under zero-field conditions and, in particular, the effects of interparticle interactions on the decay. The system is prepared in a fully aligned state in some way, and then the relaxation of its magnetization toward $\mathbf{M} = 0$ under zero-field conditions is determined. In experiments, such relaxation dynamics have been used to characterize superparamagnetic nanoparticles [28–34]. It has also been studied using Langevin-dynamics simulations, either with Néel and Brownian relaxation [38] or with Brownian relaxation only [39]. It was shown that interactions increase the relaxation time. The corresponding case of multicore magnetic particles has also been studied with simulations, and it was shown that there is a two-step relaxation process, with fast and slow relaxation times [43]. The effects of viscoelasticity of the suspending medium on the relaxation of isolated magnetic particles have also been investigated using the Fokker-Planck equation for the time-dependent, one-particle distribution function [44,55] and Brownian-dynamics (BD) simulations [44]. Interestingly, as will be shown in Sec. II B, the effects are reminiscent of those arising from interactions, although the physical situations are very different.

The relevance of magnetization relaxation to technological applications is obvious, as the relaxation time depends on the environment, as well as the particle parameters. For example, magnetorelaxometry has been exploited in designing biological immunoassays and medical theranostics with a variety of protocols [56–62]. In general, experimental results from such assays, and in characterization methods [28–34], are analyzed by ignoring the effects of interparticle interactions. The aim of the current work is to determine how interactions can modify the magnetic relaxation and to propose a theoretical basis for describing such effects.

Herein theory and simulation are applied to the case of monodisperse ferromagnetic particles undergoing Brownian relaxation. Néel relaxation is not included for two reasons. First, it increases the number of parameters and diminishes the effects of interactions, which are really the main focus of this study. Second, simulating Brownian and Néel relaxation simultaneously in a bulk system is computationally laborious due to the presence of very different characteristic timescales. Efforts have been made to simulate efficiently both types of relaxation in single particles and clusters of particles [45]. Brownian-dynamics simulations are therefore used here as idealized “experiments,” in which the nonmagnetic interactions between particles are prescribed, and complicating factors arising from polydispersity and Néel relaxation are eliminated. The simulation results are used to test the theoretical predictions derived by solving the Fokker-Planck equation for the time-dependent, one-particle orientational distribution function [23–27]. As with all such problems, a Fokker-Planck equation can be derived that governs the time evolution of a probability distribution function under the influence of random (Brownian) and drag (Stokes-Einstein) forces [63], and that includes rotational diffusion, too [23–27]. The effects of interactions between the particles are determined by introducing an effective field acting on a given particle and arising from all of the other particles. Two different approaches are taken—a first-order modified mean-field theory and a modified Weiss theory. Theory and simulation are used to show

that the effects of interactions are significant. The limits of each theory are determined by comparison to simulation, and targets for future work are identified.

The rest of this article is organized as follows. The theory is derived in Sec. II, and the BD simulation methods are detailed in Sec. III. The results are presented in Sec. IV and Sec. V concludes the article.

II. THEORY

The ferrofluid consists of N spherical particles in a volume V at temperature T . Each particle has a hard-core diameter equal to σ and carries a magnetic dipole moment $\boldsymbol{\mu}$. The potential energy of the system is $U = \sum_{i < j}^N (u_{ij}^s + u_{ij}^d)$, where u_{ij}^s is a short-range, isotropic, repulsive interaction between particles i and j and u_{ij}^d is the dipole-dipole interaction given by

$$u_{ij}^d = \frac{\mu_0}{4\pi} \left[\frac{(\boldsymbol{\mu}_i \cdot \boldsymbol{\mu}_j)}{r_{ij}^3} - \frac{3(\boldsymbol{\mu}_i \cdot \mathbf{r}_{ij})(\boldsymbol{\mu}_j \cdot \mathbf{r}_{ij})}{r_{ij}^5} \right], \quad (1)$$

where μ_0 is the vacuum permeability, $\boldsymbol{\mu}_i$ and \mathbf{r}_i are the dipole moment and position vector of particle i , and $\mathbf{r}_{ij} = \mathbf{r}_j - \mathbf{r}_i$ is the separation vector between particles i and j . The dipolar coupling constant is $\lambda = \mu_0 \mu^2 / 4\pi \sigma^3 k_B T$, where k_B is Boltzmann’s constant. The volume fraction is $\varphi = \rho v_0$, where $\rho = N/V$ is the particle concentration and $v_0 = \pi \sigma^3 / 6$ is the particle volume.

The fractional magnetization is $m(t) = M(t)/M_\infty$, where $M(t)$ is the real magnetization along the laboratory z axis, $M_\infty = N\mu/V$ is the saturation magnetization of the ferrofluid which would be achieved in an infinitely strong applied magnetic field, and t is the time. The initial, $t = 0$ state of the ferrofluid is one of perfect alignment, and hence $m(0) = 1$. The fractional magnetization can be calculated from the one-particle orientational distribution function (ODF) $W(z, t)$, where $z = \cos \theta$, and θ is the polar angle between the dipole moment on a particle and the z axis,

$$m(t) = \frac{1}{2} \int_{-1}^1 W(z, t) z dz. \quad (2)$$

The initial, $t = 0$ state of the ODF is a δ function at the point $z = 1$, since the angle $\theta = 0$ for each particle’s dipole moment. This initial ODF can be expressed as an expansion in terms of Legendre polynomials $P_k(z)$,

$$W(z, 0) = \sum_{k=0}^{\infty} (2k+1) P_k(z). \quad (3)$$

From $t = 0$ the magnetization is allowed to relax. In the following sections, three different levels of theory are detailed: the theory for noninteracting particles (Sec. II A), a modified mean-field theory for interacting particles (Sec. II B), and a modified Weiss theory for interacting particles (Sec. II C).

A. Noninteracting particles

The time dependence of the ODF is governed by the Fokker-Planck (FP) equation, simplified in the present case because only the z component of the magnetization is of interest, and hence the relevant ODF depends only on the polar

angle θ [Eq. (2)]. For ideal, noninteracting particles, the FP equation is [23–27]

$$\begin{aligned} 2\tau_B \frac{\partial W_{\text{id}}}{\partial t} &= \nabla^2 W_{\text{id}} \\ &= \frac{1}{\sin \theta} \frac{\partial}{\partial \theta} \left(\sin \theta \frac{\partial W_{\text{id}}}{\partial \theta} \right) \\ &= \frac{\partial}{\partial z} \left[(1 - z^2) \frac{\partial W_{\text{id}}}{\partial z} \right], \end{aligned} \quad (4)$$

where τ_B is the Brownian rotation time. For spherical particles, the Stokes-Einstein-Debye relationship is $\tau_B = \pi \eta \sigma^3 / 2k_B T$, where η is the viscosity of the suspending liquid. The solution of Eq. (4) is evidently

$$W_{\text{id}}(z, t) = \sum_{k=0}^{\infty} (2k+1) P_k(z) \exp \left[-\frac{k(k+1)t}{2\tau_B} \right], \quad (5)$$

and it gives a simple exponential relaxation law for the magnetization, with the $k=1$ term being the only one that contributes to m :

$$m_{\text{id}}(t) = \exp \left(-\frac{t}{\tau_B} \right). \quad (6)$$

In Secs. II B and II C, interactions will be included in the FP equation. In earlier work, two related approaches have been proposed and tested for static and dynamic properties at or near to equilibrium: the so-called modified mean-field theory and modified Weiss theory.

B. Modified mean-field theory for interacting particles

For interacting particles, the FP equation can be written [23–27]

$$2\tau_B \frac{\partial W}{\partial t} = \frac{\partial}{\partial z} \left[(1 - z^2) \left(\frac{\partial W}{\partial z} + \frac{W}{k_B T} \frac{\partial U_{\text{eff}}}{\partial z} \right) \right], \quad (7)$$

where U_{eff} is the effective interaction energy between a particle and all of the other particles in the system. The stationary, equilibrium distribution is $W(z) = \exp[-U_{\text{eff}}(z)/k_B T]$. In the first-order dynamic modified mean-field (MMF) model [48], U_{eff} is approximated by an expression which is linear in the particle concentration ρ . Each randomly chosen particle interacts with the total dipolar magnetic field \mathbf{H}_{MMF} produced by all of the other particles in the system [see Eq. (1)], but no spatial or orientational correlations between particles are taken into account. U_{eff} is given by

$$\frac{U_{\text{eff}}}{k_B T} = -\frac{\mu_0(\boldsymbol{\mu} \cdot \mathbf{H}_{\text{MMF}})}{k_B T}, \quad (8)$$

with an effective field given by

$$\begin{aligned} \mathbf{H}_{\text{MMF}} &= \frac{\rho}{4\pi} \int_{r_{12} \geq \sigma} d\mathbf{r}_{12} \int d\boldsymbol{\mu}_2 W_{\text{id}}(z_2, t) \\ &\quad \times \left[\frac{\boldsymbol{\mu}_2}{r_{12}^3} - \frac{3\mathbf{r}_{12}(\boldsymbol{\mu}_2 \cdot \mathbf{r}_{12})}{r_{12}^5} \right]. \end{aligned} \quad (9)$$

In this term, the integration over all possible positions and orientations of particle 2 is weighted by the ODF for noninteracting particles, i.e., W_{id} from Eq. (5). Carrying out the integration gives

$$\frac{U_{\text{eff}}}{k_B T} = -\chi_L \exp \left(-\frac{t}{\tau_B} \right) z, \quad (10)$$

where $\chi_L = \rho \mu_0 \mu^2 / 3k_B T = 8\varphi \lambda$ is the Langevin magnetic susceptibility of an ideal paramagnetic gas. The solution of Eqs. (7) and (10) is expressed as a sum of Legendre polynomials by

$$W_{\text{MMF}}(z, t) = \sum_{k=0}^{\infty} (2k+1) A_k(t) P_k(z), \quad (11)$$

where $A_0(t) = 1$, $A_k(0) = 1$, and from Eq. (2), the fractional magnetization is $m_{\text{MMF}}(t) = A_1(t)$. Matching terms with the same $P_k(z)$ gives a set of equations for the coefficients $A_k(t)$,

$$\frac{2\tau_B}{k(k+1)} \frac{dA_k}{dt} = -\left[A_k + \frac{\chi_L}{2k+1} e^{-t/\tau_B} (A_{k+1} - A_{k-1}) \right]. \quad (12)$$

Since the interaction term U_{eff} is linear in the particle concentration ρ , it is appropriate to solve the set of equations for A_1 to the same accuracy, meaning linear in χ_L . Therefore, the time dependence of A_2 is approximated by

$$\tau_B \frac{dA_2}{dt} = -3A_2 + \mathcal{O}(\chi_L), \quad (13)$$

and hence $A_2(t) = \exp(-3t/\tau_B)$. At this level of approximation, the time dependence of A_1 becomes

$$\tau_B \frac{dA_1}{dt} = -A_1 - \frac{\chi_L}{3} e^{-t/\tau_B} (e^{-3t/\tau_B} - 1). \quad (14)$$

Thus, the MMF solution for the fractional magnetization is

$$\begin{aligned} m_{\text{MMF}}(t) &= \exp \left(-\frac{t}{\tau_B} \right) \\ &\quad \times \left\{ 1 + \frac{\chi_L}{3} \left[\frac{t}{\tau_B} + \frac{1}{3} (e^{-3t/\tau_B} - 1) \right] \right\}. \end{aligned} \quad (15)$$

So the main exponential decay remains the same, but it is attenuated by a term arising from the interparticle interaction. The initial relaxation of the MMF solution coincides with that for noninteracting particles [Eq. (6)].

At this point, the apparent similarity between Eq. (15) and a result from Ref. [44] is highlighted. In Ref. [44], the Brownian motion of noninteracting nanoparticles in a viscoelastic, Maxwell material was derived from the appropriate Fokker-Planck equation. The Maxwell material is characterized by a retarded friction coefficient, $\zeta(t)$, which gives the drag arising from the relative motion of the particle and the surrounding medium, and is given by $\zeta(t) = (\zeta_0/\tau_M) \exp(-t/\tau_M)$, where τ_M is the Maxwell relaxation time. Denoting the Brownian friction coefficient as $\xi = 2k_B T \tau_B$, the parameter $q = \zeta_0/\xi$ controls the ratio of elastic to viscous friction. Obviously, the current situation corresponds to the limit $q \rightarrow 0$, as was pointed out in Ref. [44]. Nonetheless, using a similar approximation to that employed here, the magnetic relaxation

in the viscoelastic case gives a function identical to Eq. (15) except that $\chi_L/3$ is replaced by q , and in the second term in square brackets, the prefactor of $1/3$ becomes τ_M/τ_B , and τ_B in the exponent becomes $3\tau_M$. But it must be understood that although the final equations are of similar form, the physical origin is completely different: in Ref. [44], the form of $m(t)$ arises from the viscoelasticity of the Maxwell medium on the relaxation of a single particle; in Eq. (15), it arises from the magnetic interactions between all of the particles suspended in a Newtonian fluid.

The first-order MMF approach—embodied by Eq. (10)—has been tested many times using experimental data and computer simulations both for static and dynamic magnetic properties. The main conclusion is that this simple approach gives a very good description of the effects of interactions, but the range of validity is limited to $\chi_L < 3$ for static properties such as the magnetization curve and initial susceptibility [10–12], and $\chi_L < 1$ for the dynamic initial magnetic susceptibility [40–42].

C. Modified Weiss theory for interacting particles

An improved method which expands the range of validity of the MMF approach was suggested recently [41] and is similar to the Weiss mean-field theory [2]. In this approach, the total magnetic field \mathbf{H}_{MMF} acting on a randomly chosen particle, and arising from all of the other particles, is determined as in Eq. (9) but with $W(z_2, t)$ determined self-consistently,

$$\begin{aligned} \frac{U_{\text{eff}}}{k_B T} &= -\frac{\mu_0(\boldsymbol{\mu} \cdot \mathbf{H}_W)}{k_B T} \quad (16) \\ \mathbf{H}_W &= \frac{\rho}{4\pi} \int_{r_{12} \geq \sigma} d\mathbf{r}_{12} \int d\boldsymbol{\mu}_2 W(z_2, t) \\ &\quad \times \left[\frac{\boldsymbol{\mu}_2}{r_{12}^3} - \frac{3\mathbf{r}_{12}(\boldsymbol{\mu}_2 \cdot \mathbf{r}_{12})}{r_{12}^5} \right]. \quad (17) \end{aligned}$$

Now $W(z_2, t)$ is the *unknown* ODF of the second particle. Expanding the ODF as a sum of Legendre polynomials gives

$$W(z, t) = \sum_{k=0}^{\infty} (2k+1) B_k(t) P_k(z), \quad (18)$$

where $B_0(t) = 1$, $B_k(0) = 1$, and from Eq. (2), the fractional magnetization is $m(t) = B_1(t)$. Combining Eqs. (16)–(18) gives

$$\frac{U_{\text{eff}}}{k_B T} = -\chi_L B_1 z. \quad (19)$$

Substitution of this expression into Eq. (7), and matching terms with the same $P_k(z)$, leads to the following set of equations for the coefficients B_k :

$$\frac{dB_k}{dt} = -\frac{k(k+1)}{2\tau_B} \left[B_k + \frac{\chi_L}{2k+1} B_1 (B_{k+1} - B_{k-1}) \right]. \quad (20)$$

It is important to note that all of the coefficients depend on the first one, B_1 , this being equal to the fractional magnetization m . The time dependence of the magnetization in the self-consistent Weiss approach (16) is therefore given by

$$\tau_B \frac{dm_W}{dt} = -\left(1 - \frac{\chi_L}{3} + \frac{\chi_L}{3} B_2\right) m_W. \quad (21)$$

To keep this equation at linear order in χ_L , the time dependence of B_2 can be approximated by

$$\tau_B \frac{dB_2}{dt} = -3B_2 + \mathcal{O}(\chi_L), \quad (22)$$

and hence $B_2(t) = \exp(-3t/\tau_B)$. For $\chi_L \geq 3$, Eq. (21) predicts an instantaneous rate $d \ln m_W/dt > 0$ at long times, which is clearly nonphysical. This is related to the well-known artifact of the Weiss mean-field theory, which is a transition to a long-range-ordered state at $\chi_L = 3$. An approximate equation for m which is close to the Weiss mean-field theory, but which does not exhibit a pathological transition, is

$$\tau_B \frac{dm_{\text{MW}}}{dt} = -\left(1 + \frac{\chi_L}{3} - \frac{\chi_L}{3} e^{-3t/\tau_B}\right)^{-1} m_{\text{MW}}. \quad (23)$$

This expression preserves higher-order terms in χ_L representing interactions, but at all times, $d \ln m_{\text{MW}}/dt \leq 0$. We call the result of changing Eq. (21) to Eq. (23) the “modified Weiss” (MW) model, and this model was thoroughly tested in Ref. [41] against computer simulations of the dynamic magnetic susceptibility, $\chi(\omega)$. Integrating Eq. (23) gives

$$m_{\text{MW}}(t) = \exp \left\{ -\frac{3t/\tau_B + \ln[1 + \chi_L(1 - e^{-3t/\tau_B})/3]}{3 + \chi_L} \right\}. \quad (24)$$

It is clear from Eq. (23) that the initial decay is independent of interactions, with $d \ln m_{\text{MW}}/dt \approx -1/\tau_B$, and hence

$$m_{\text{MW}}(t) \approx \exp\left(-\frac{t}{\tau_B}\right) \quad (t \rightarrow 0). \quad (25)$$

For long times, when $t \gg \tau_B/3$, the relaxation becomes interaction dependent, with an asymptotic exponential decay time equal to $(1 + \chi_L/3)\tau_B$,

$$m_{\text{MW}}(t) \approx \exp \left\{ -\frac{3t/\tau_B + \ln[1 + \chi_L/3]}{3 + \chi_L} \right\} \quad \left(t \gg \frac{\tau_B}{3}\right). \quad (26)$$

The asymptotic behavior of the MW model (24) with weak interactions (meaning $\chi_L \ll 3$) coincides with the MMF prediction (15).

III. SIMULATIONS

Brownian-dynamics simulations were carried out using LAMMPS [64,65]. Spherical particles ($N = 1728$) with central point dipoles were simulated in a cubic simulation box with periodic boundary conditions applied. The long-range dipolar interactions were computed with the particle-particle, particle-mesh method [66], and the short-range interactions u_{ij}^s were given by the purely repulsive Weeks-Chandler-Andersen potential [67]. In Lennard-Jones (LJ) units, the reduced temperature was $T^* = k_B T/\epsilon = 1$, where ϵ is the LJ well depth, the dipolar coupling constant was $\lambda = (\mu^*)^2/T^*$, where μ^* is the reduced dipole moment, and the particle volume fraction was φ . BD were generated by integrating the Langevin equation with a large-enough friction coefficient ξ so that the short-time inertial dynamics are suppressed. In LAMMPS, this is controlled with the damping time $t_{\text{damp}}^* \propto 1/\xi$ and the corresponding Brownian rotation time $\tau_B^* = 1/6T^* t_{\text{damp}}^*$, both in LJ units [40]. In earlier work on

equilibrium magnetization fluctuations and the dynamic magnetic susceptibility, $t_{\text{damp}}^* = 1/20$ ($\tau_B^* = 10/3$) was sufficiently small to ensure that the correlation function $\langle \mathbf{M}(t) \cdot \mathbf{M}(0) \rangle$ for noninteracting particles was equal to $\langle M^2 \rangle \exp(-t/\tau_B)$ at all times, as expected for Brownian motion [40]. In the current work, $t_{\text{damp}}^* = 1/60$ ($\tau_B^* = 10$), which is more than adequate to ensure that $m(t)$ for noninteracting particles is equal to the exact result given by Eq. (6); this will be shown explicitly in Sec. IV. This simulation approach was taken to exploit the functionality of LAMMPS, which does not have a dedicated BD routine. In LJ units, the integration time step was $\delta t^* = 0.005$. Simulations were carried out according to three different protocols.

(i) In *method A* the system was equilibrated in zero applied field. Then all dipole moments were set equal to $(0, 0, \mu^*)$, and the relaxation dynamics were simulated. Some structures such as chains or rings can form in the fluid prior to the alignment and relaxation of the dipoles, particularly with large values of λ .

(ii) In *method B* the system was equilibrated with the dipolar interactions switched off, so that there were no spatial or orientational correlations between particles. Then all dipole moments were set equal to $(0, 0, \mu^*)$, the interactions were turned on, and the relaxation dynamics were simulated. This protocol was studied to see if it agreed better with the no-correlation approximation made in Eqs. (9) and (17) is justified.

(iii) In *method C* the system was equilibrated with all of the dipole moments constrained to $(0, 0, \mu^*)$, corresponding to a strong aligning field. With large values of λ , and at low concentrations, the particles formed distinct chains aligned along the z direction. Then the orientational constraint was removed, and the relaxation dynamics were simulated.

Method C corresponds to the most common type of magnetorelaxometry experiments [28–34]. Method A could be realized in a pulsed-field experiment, as long as the pulse width is short compared to the typical structural and orientational relaxation times and the field intensity is high enough to overcome the interactions between particles and orient them all in the same direction. Method B is the most artificial, but as already mentioned, it is of theoretical interest. Simulations with $\varphi = 0.125$ and $\lambda = 1, 2, 3$, and 4 were carried out using methods A, B, and C. Simulations with $\lambda = 1$ and $\varphi = 0.125, 0.250, 0.375$, and 0.500 were carried out using methods A and B. Simulations with $\varphi = 0.010$ and $\lambda = 1, 2, 3, 4$, and 8 were carried out using methods A and C. The rationale for these choices of method will be given as the results are presented in Sec. IV. Simulations were also carried out without any interactions between particles, just to test the simulation protocol. For each method and set of parameters, 20 independent simulations were carried out using different disordered initial configurations and different random number generator seeds.

IV. RESULTS

Figure 1 shows $m(t)$ from simulations using methods A, B, and C for systems with volume fraction $\varphi = 0.125$ and $\lambda = 1-4$, along with the theoretical predictions of Eqs. (15) and (24). For reference, simulation and theoretical results for systems without interparticle interactions are also shown; in

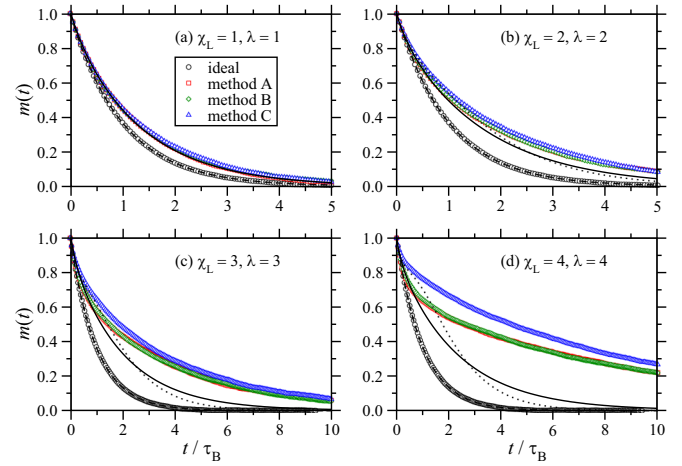


FIG. 1. The fractional magnetization as a function of time in systems with $\varphi = 0.125$: (a) $\chi_L = 1$ and $\lambda = 1$; (b) $\chi_L = 2$ and $\lambda = 2$; (c) $\chi_L = 3$ and $\lambda = 3$; and (d) $\chi_L = 4$ and $\lambda = 4$. The points are from simulations: black circles are for noninteracting particles; red squares are from method A; green diamonds are from method B; and blue up-triangles are from method C. The lines are from theory: the dashed lines are for noninteracting particles [Eq. (6)], and they lie perfectly on top of the simulation points; the dotted lines are from MMF theory for interacting particles [Eq. (15)]; and the solid lines are from MW theory for interacting particles [Eq. (24)].

this case, Eq. (6) holds true, and the agreement between theory and simulation is perfect (the dashed lines from theory lie exactly on top of the simulation points). Note the different time ranges for $\lambda \leq 2$ and $\lambda \geq 3$. The simulation results from methods A and B are practically identical for each value of λ , meaning that the no-correlation approximation made in Eqs. (9) and (17) is justified in calculating the magnetization decay. Of course, there are significant, short-range spatial and orientational correlations with such parameters, as was shown in detail in Ref. [68], and correlations can build up during the magnetization-relaxation process. But in the present calculations, the long-range nature of the dipolar interaction suggests that the contributions of the short-range correlations to the effective field are not essential. Method C only gives significantly different results from methods A and B when $\lambda = 4$, and shows a higher magnetization and, at intermediate times $t \sim \tau_B$, a slower decay. In method C, the initial configuration is equilibrated with perfect alignment of the particle dipoles, which favors chainlike correlations with large values of λ . Hence, the slower decay of the magnetization is due to long-lived chains of particles. With smaller values of λ , the particle interactions are not strong enough to stabilize chainlike correlations, and hence the results from methods A, B, and C are all very similar. In general, the decay rate decreases with increasing λ due to sustained orientational correlations between the particle dipoles; with $\lambda = 1$, $m(t)$ decays to $1/e$ in a time $t \simeq \tau_B$, while with $\lambda = 4$, this time is approximately an order of magnitude larger. The decay time will be considered in more detail below.

The MW theory is accurate with $\lambda = 1$, but the deviation from simulation grows with increasing λ . With $\lambda = 1$, there is a significant difference between the predictions for systems with and without interactions, and the effects of interactions

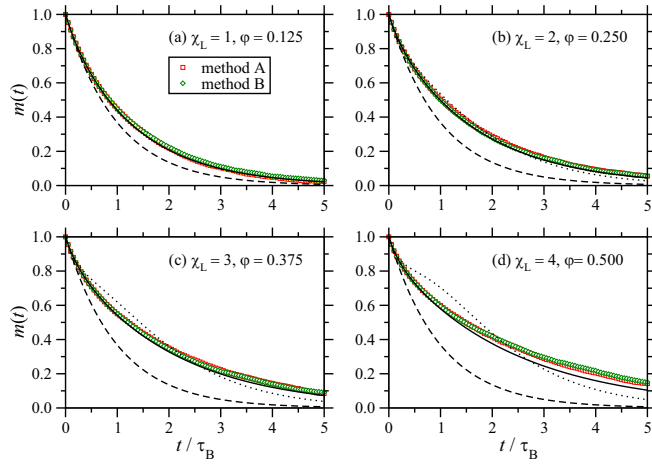


FIG. 2. The fractional magnetization as a function of time in systems with $\lambda = 1$: (a) $\chi_L = 1$ and $\varphi = 0.125$; (b) $\chi_L = 2$ and $\varphi = 0.250$; (c) $\chi_L = 3$ and $\varphi = 0.375$; and (d) $\chi_L = 4$ and $\varphi = 0.500$. The points are from simulations: red squares are from method A and green diamonds are from method B. The lines are from theory: the dashed lines are for noninteracting particles [Eq. (6)]; the dotted lines are from MMF theory for interacting particles [Eq. (15)]; and the solid lines are from MW theory for interacting particles [Eq. (24)].

are clearly captured well, as shown by the agreement with simulations. The MW theory predicts that the asymptotic decay time increases with increasing λ , given by $(1 + \chi_L/3)\tau_B$, but this is not as rapid an increase as that seen in simulations. The MMF theory coincides with the MW theory when $\chi_L = 1$, but there are large deviations with stronger interactions. Moreover, the MMF curve incorrectly predicts nonmonotonic behavior at times $t \gtrsim \tau_B$.

Because $\lambda = 1$ is within the range of validity of the theory, a comparison between simulation and theory is next made with increasing φ . The simulations were carried out with methods A and B, as chain formation is not expected to be significant at high concentrations. Figure 2 shows the results. Methods A and B give essentially identical results, showing that even at high concentration where short-range correlations are more pronounced [68], the effects on the magnetization decay are insignificant. Of course, in method B, correlations can build up during the magnetization-relaxation process.

The agreement between simulation and MW theory is very good, even at the highest volume fraction $\varphi = 0.500$. So the MW theory is accurate up to $\chi_L = 4$, as long as λ is not too large. This highlights the role of chainlike correlations in the magnetization-relaxation process: with small φ and large λ , chainlike correlations will be enhanced, and the theory is inaccurate; with large φ and small λ , the theory is accurate. As in the $\varphi = 0.125$ case, the MMF theory is valid for $\chi_L = 1$, but it is incorrect for higher values.

To highlight the effect of chain formation, systems with $\varphi = 0.010$ are now considered. With small values of λ , the decay should be almost ideal. With large values of $\lambda \geq 4$ [69–71], chain formation should lead to very slow decay of the magnetization. Snapshots of systems with $\varphi = 0.010$ and $\lambda = 2, 4$, and 8 are shown in Fig. 3, comparing the initial configurations from methods A and C. These show the extent of chain formation and alignment with large values of λ . With

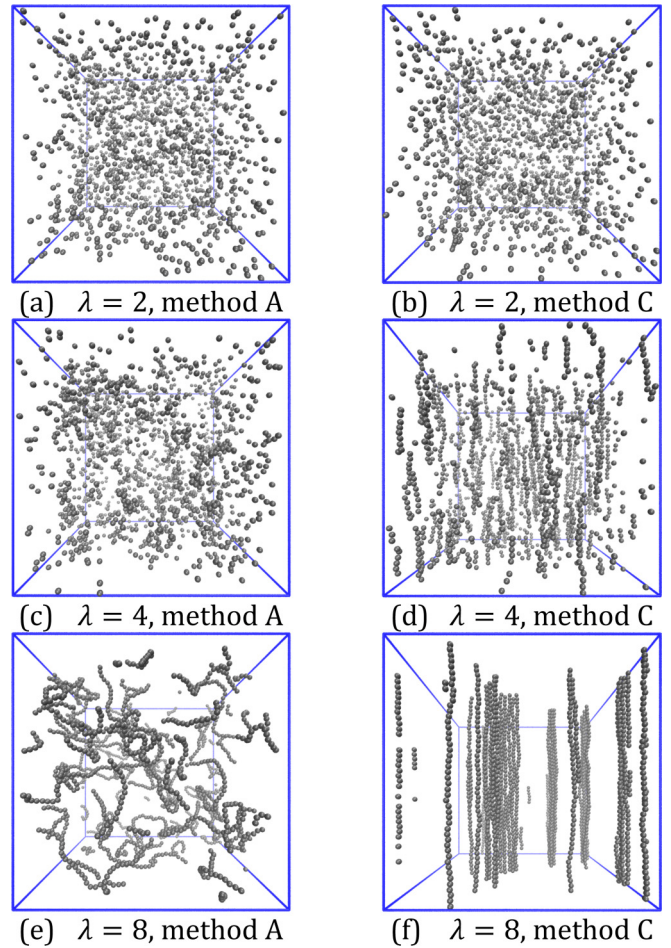


FIG. 3. Snapshots of the initial configurations of systems with $\varphi = 0.010$ from method A [(a), (c), and (e)] and method C [(b), (d), and (f)]: (a) $\lambda = 2$, method A; (b) $\lambda = 2$, method C; (c) $\lambda = 4$, method A; (d) $\lambda = 4$, method C; (e) $\lambda = 8$, method A; and (f) $\lambda = 8$, method C. In each case, the particle dipole moments relax from perfect alignment in the vertical direction.

$\lambda \leq 2$, there is no discernible structure arising from either method. With $\lambda = 4$, there are small clusters in method A, and short, parallel chains in method C. With $\lambda = 8$, method A gives long chains and some rings, and method C gives thick ropes aligned in the same direction of the particle dipole moments (and a field).

To put this on a quantitative basis, Fig. 4 shows the equilibrium cluster-size distribution p_n before relaxation, with clusters of size n identified with a simple distance-based cut-off with $r_c = 1.4\sigma$. This distance corresponds to the local minimum between the first and second peaks in the radial distribution function. In both methods A and C, p_n looks to be approximately exponential at large n , which is the prediction of many simple clustering models [72]. The distribution extends to larger n with increasing λ , and the mean value $\langle n \rangle$ grows accordingly, as shown in the figure legend. In addition, method C (corresponding to a strong aligning field) gives rise to larger clusters than method A. With $\lambda = 8$, some clusters are system spanning, the number of clusters is too small to give a meaningful estimate of p_n , and hence the results are not shown; nonetheless, rough estimates of the mean cluster size

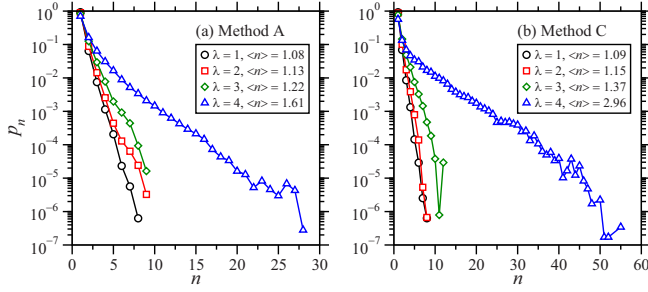


FIG. 4. Equilibrium cluster-size distributions before relaxation in the systems with $\varphi = 0.010$ from method A (a) and method C (b). The mean values $\langle n \rangle$ are shown for $\lambda = 1, 2, 3$, and 4 . Results for $\lambda = 8$ are omitted, because the clusters become too large, but the mean cluster sizes are $\langle n \rangle \simeq 90$ (method A) and $\langle n \rangle \simeq 110$ (method C).

are $\langle n \rangle \simeq 90$ (method A) and $\langle n \rangle \simeq 110$ (method C). The extent of clustering is anyway obvious from Figs. 3(e) and 3(f).

Relaxation results for systems with $\lambda = 1, 2, 4$, and 8 are shown in Fig. 5. Note the logarithmic scale on the abscissa. With $\lambda = 1$ ($\chi_L = 0.08$) and $\lambda = 2$ ($\chi_L = 0.16$), the decay is essentially ideal, simulations with methods A and C give the same results, and the agreement between simulation and all theories is excellent. Because χ_L is so small, the ideal, MMF, and MW theories are all quite similar, and the MMF and MW theories are virtually indistinguishable. With $\lambda = 4$, method C gives a much slower decay than with method A, due to the formation of chains by perfectly aligned particles. Both methods give a much slower decay than that predicted by theory; even though the Langevin susceptibility is small, the strong interactions between particles are outwith the regime of

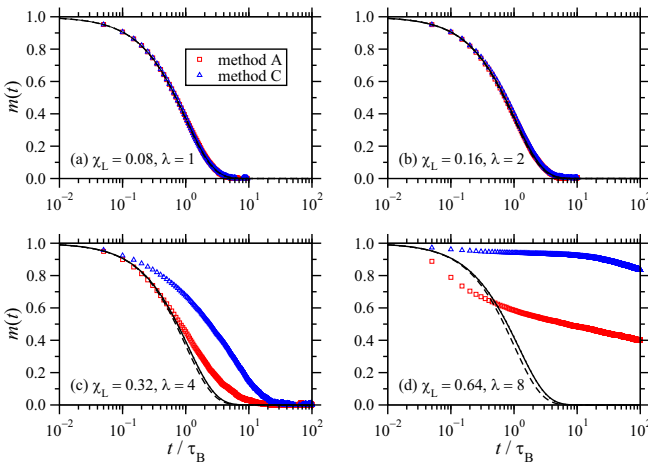


FIG. 5. The fractional magnetization as a function of time in systems with $\varphi = 0.010$: (a) $\chi_L = 0.08$ and $\lambda = 1$; (b) $\chi_L = 0.16$ and $\lambda = 2$; (c) $\chi_L = 0.32$ and $\lambda = 4$; and (d) $\chi_L = 0.64$ and $\lambda = 8$. The points are from simulations: red squares are from method A and blue up-triangles are from method C. The lines are from theory: the dashed lines are for noninteracting particles [Eq. (6)]; the dotted lines are from MMF theory for interacting particles [Eq. (15)]; and the solid lines are from MW theory for interacting particles [Eq. (24)]. The dotted and solid lines (MMF and MW theories, respectively) are indistinguishable on the scale of the plot.

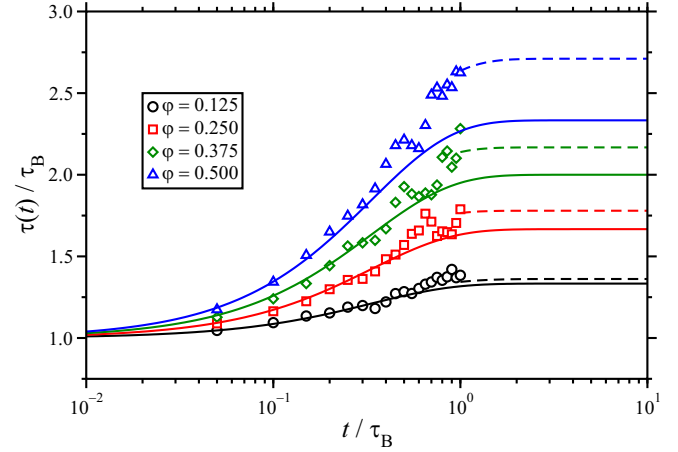


FIG. 6. Instantaneous decay times, as defined in Eq. (27), for systems with $\lambda = 1$ and $\varphi = 0.125, 0.250, 0.375$, and 0.500 . The points are from simulations with method A. The dashed lines are obtained from fits to the simulation data for $t \geq \tau_B$. The solid lines are from Eqs. (24) and (27).

validity of the theories. The same behavior is seen with $\lambda = 8$, although the simulated decay is orders of magnitude slower than with $\lambda = 4$, and this was not simulated to completion. Method A gives a much more rapid initial decay than method C. This is because, initially, the particles are all strongly clustered into chains and rings. On aligning the dipole moments, there will be repulsions between particles in those chains or ring segments that are not oriented in the z direction. In method C, the particles are strongly aligned into ropes, and at the start of the magnetization-relaxation process, there are strong attractive interactions between particles, leading to a much slower initial decay.

Overall, the MW gives the best agreement with simulation. Equations (25) and (26) give predictions for the short-time and long-time exponential behavior of $m(t)$, and there should be a crossover at intermediate times. To characterize this crossover, an instantaneous decay time can be defined by

$$\tau(t) = -\left(\frac{d \ln m}{dt}\right)^{-1}. \quad (27)$$

To evaluate this quantity from simulation data, a two-part process was followed. For short times, meaning $t < \tau_B$, the magnetization is still sufficiently high that it is possible to calculate $\tau(t)$ by finite differences. For longer times, the finite-difference method gives very noisy results. Therefore, to estimate the asymptotic decay time, Eq. (24) was fitted to $m(t)$ in the range $t \geq \tau_B$, but with adjustable parameters in place of τ_B and χ_L . $\tau(t)$ was then obtained from Eq. (27). To summarize, the simulations were run for times much longer than τ_B , but a fit to the data in this regime gives a more reliable estimate of the instantaneous decay time $\tau(t)$ than using finite differences.

Figure 6 shows the results for systems with $\lambda = 1$. The simulation results are from method A only. In all cases, the instantaneous decay time at short times is equal to τ_B , as predicted by Eq. (25). The MW theory is reasonably good at all times, even with $\varphi = 0.500$.

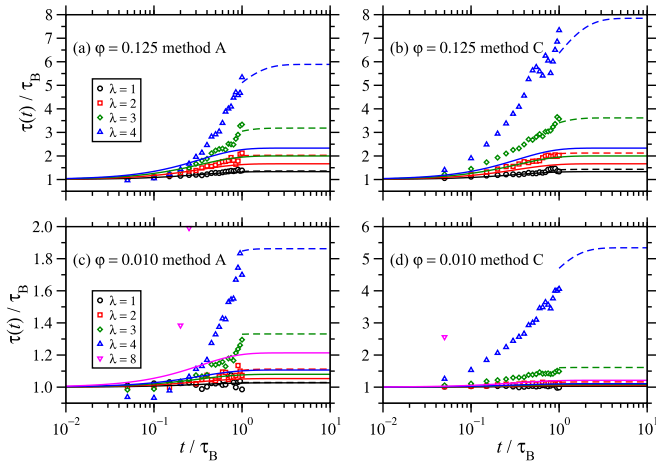


FIG. 7. Instantaneous decay times, as defined in Eq. (27): [(a) and (b)] systems with $\varphi = 0.125$ and $\lambda = 1, 2, 3,$ and 4 ; [(c) and (d)] systems with $\varphi = 0.010$ and $\lambda = 1, 2, 3, 4,$ and 8 . In (a) and (c) the points are from simulations with method A. In (b) and (d) the points are from simulations method C. The dashed lines are obtained from fits to the simulation data for $t \geq \tau_B$. The solid lines are from Eqs. (24) and (27).

Figure 7 shows the results for systems with $\varphi = 0.125$ and 0.010 . For both volume fractions, the asymptotic decay times from simulations with method C are larger than those with method A, due to the extent of chain formation before the magnetization-relaxation process. With $\varphi = 0.125$ [Figs. 7(a) and 7(b)] the MW theory is only accurate with $\lambda = 1$. With $\varphi = 0.010$ [Figs. 7(c) and 7(d)], the MW theory is accurate for $\lambda = 1$ and 2 , where the decay is essentially ideal, while in the chain-formation regime ($\lambda \geq 4$), the asymptotic decay time is orders of magnitude larger than predicted. For $\lambda = 8$, the decay is so slow that it was not possible to fit or extrapolate the asymptotic decay. Nonetheless, in all cases, the initial decay is “ideal,” with $\tau \approx \tau_B$.

V. CONCLUSIONS

The dynamics of magnetization relaxation in ferrofluids has been studied using theory and Brownian dynamics simulations. The theory was based on solving the Fokker-Planck equation for the one-particle orientational distribution function. Interactions were included with an effective magnetic

field acting on a given particle due to all of the other particles. Two different approximations were proposed—a first-order modified mean-field theory and a modified Weiss theory. The simulations were carried out according to various protocols with different initial conditions: ideal, noncorrelated configurations; configurations in zero-field conditions; and configurations with an infinitely strong field. In all cases, the magnetization was instantaneously set to its saturation value, and then its relaxation was simulated.

With moderate values of the dipolar coupling constant ($\lambda = 1$), the modified Weiss theory gives an excellent description of the magnetization relaxation. With stronger interactions, and dipolar coupling constants up to $\lambda = 8$, there are increasing deviations between theory and simulation. This is due to the presence of growing chainlike spatial and orientational correlations between particles.

The theory predicts a crossover in instantaneous relaxation times: at short times ($t \lesssim 0.1\tau_B$), the initial decay is characterized by the Brownian relaxation time and is unaffected by interactions; at long times, the asymptotic decay depends on the interaction strength; and in between, there is a smooth crossover. Compared to simulations, the theoretical predictions are accurate with $\lambda = 1$, but with stronger interactions, the asymptotic decay time is significantly underestimated. Nonetheless, the prediction that the initial decay is always “ideal,” with a decay time τ_B , is supported by the simulation data.

Overall, the theory should be reliable for real ferrofluids with dipolar coupling constants $\lambda \sim 1$. The theory breaks down when the interactions between particles are strong enough for chain formation. The extension of the theory to the chaining regime is a topic for future study, but the main challenge will be to incorporate the time evolution of the cluster distribution, and the effective fields felt by particles within clusters of various sizes and structures. Another interesting topic is the role of polydispersity, which introduces complexity in the cluster distribution [73], and the spread of relaxation times and interaction strengths [41].

ACKNOWLEDGMENTS

A.O.I. gratefully acknowledges research funding from the Ministry of Science and Higher Education of the Russian Federation (Contract No. 02.A03.21.006, Ural Mathematical Center Project No. 075-02-2020-1537/1).

- [1] R. E. Rosensweig, *Ferrohydrodynamics* (Dover, New York, 1998).
- [2] P. Weiss, *J. Phys. Theor. Appl.* **6**, 661 (1907).
- [3] A. Tsebers, *Magneto hydrodynamics* **18**, 137 (1982).
- [4] M. S. Wertheim, *J. Chem. Phys.* **55**, 4291 (1971).
- [5] K. I. Morozov and A. V. Lebedev, *J. Mag. Mag. Mater.* **85**, 51 (1990).
- [6] A. F. Pshenichnikov, A. V. Lebedev, and K. I. Morozov, *Magneto hydrodynamics* **23**, 31 (1987).
- [7] Yu. A. Buyevich and A. O. Ivanov, *Physica A* **190**, 276 (1992).
- [8] A. F. Pshenichnikov and A. V. Lebedev, *Colloid J.* **57**, 800 (1995).
- [9] A. F. Pshenichnikov, V. V. Mekhonoshin, and A. V. Lebedev, *J. Mag. Magn. Mater.* **161**, 94 (1996).
- [10] A. O. Ivanov and O. B. Kuznetsova, *Phys. Rev. E* **64**, 041405 (2001).
- [11] A. O. Ivanov and O. B. Kuznetsova, *Colloid J.* **63**, 60 (2001).
- [12] A. O. Ivanov, S. S. Kantorovich, E. N. Reznikov, C. Holm, A. F. Pshenichnikov, A. V. Lebedev, A. Chremos, and P. J. Camp, *Phys. Rev. E* **75**, 061405 (2007).
- [13] A. Yu. Solovyova, E. A. Elfimova, A. O. Ivanov, and P. J. Camp, *Phys. Rev. E* **96**, 052609 (2017).
- [14] B. Huke and M. Lücke, *Phys. Rev. E* **62**, 6875 (2000).
- [15] B. Huke and M. Lücke, *Phys. Rev. E* **67**, 051403 (2003).

- [16] I. Szalai and S. Dietrich, *J. Phys.: Condens. Matter* **20**, 204122 (2008).
- [17] I. Szalai and S. Dietrich, *J. Phys.: Condens. Matter* **23**, 326004 (2011).
- [18] I. Szalai, S. Nagy, and S. Dietrich, *J. Phys.: Condens. Matter* **25**, 465108 (2013).
- [19] I. Szalai, S. Nagy, and S. Dietrich, *Phys. Rev. E* **92**, 042314 (2015).
- [20] R. E. Rosensweig, *J. Mag. Magn. Mater.* **252**, 370 (2002).
- [21] Q. A. Pankhurst, J. Connolly, S. K. Jones, and J. Dobson, *J. Phys. D: Appl. Phys.* **36**, R167 (2003).
- [22] Q. A. Pankhurst, N. T. K. Thanh, S. K. Jones, and J. Dobson, *J. Phys. D: Appl. Phys.* **42**, 224001 (2009).
- [23] W. F. Brown, Jr., *J. Appl. Phys.* **34**, 1319 (1963).
- [24] W. F. Brown, Jr., *Phys. Rev.* **130**, 1677 (1963).
- [25] W. F. Brown, Jr., *IEEE Trans. Magn.* **15**, 1196 (1979).
- [26] M. A. Martsenyuk, Yu. L. Raikher, and M. I. Shliomis, *Zh. Eksp. Teor. Fiz.* **65**, 834 (1974) [*Sov. Phys. JETP* **38**, 413 (1974)].
- [27] Yu. L. Raikher and M. I. Shliomis, *Zh. Eksp. Teor. Fiz.* **67**, 1060 (1975) [*Sov. Phys. JETP* **40**, 526 (1975)].
- [28] D. Eberbeck, S. Hartwig, U. Steinhoff, and L. Trahms, *Magneto hydrodynamics* **39**, 77 (2003).
- [29] F. Ludwig, S. Mäuselein, E. Heim, and M. Schilling, *Rev. Sci. Instrum.* **76**, 106102 (2005).
- [30] D. Eberbeck, F. Wiekhorst, U. Steinhoff, and L. Trahms, *J. Phys.: Condens. Matter* **18**, S2829 (2006).
- [31] F. Ludwig, E. Heim, D. Menzel, and M. Schilling, *J. Appl. Phys.* **99**, 08P106 (2006).
- [32] F. Ludwig, E. Heim, and M. Schilling, *J. Appl. Phys.* **101**, 113909 (2007).
- [33] J. Dieckhoff, D. Eberbeck, M. Schilling, and F. Ludwig, *J. Appl. Phys.* **119**, 043903 (2016).
- [34] J. Fock, C. Balceris, R. Costo, L. Zeng, F. Ludwig, and M. F. Hansen, *Nanoscale* **10**, 2052 (2018).
- [35] A. O. Ivanov, S. S. Kantorovich, V. S. Zverev, E. A. Elfimova, A. V. Lebedev, and A. F. Pshenichnikov, *Phys. Chem. Chem. Phys.* **18**, 18342 (2016).
- [36] A. V. Lebedev, V. I. Stepanov, A. A. Kuznetsov, A. O. Ivanov, and A. F. Pshenichnikov, *Phys. Rev. E* **100**, 032605 (2019).
- [37] P. Lemal, S. Balog, L. Ackermann-Hirschi, P. Taladriz-Blanco, A. M. Hirt, B. Rothen-Rutishauser, M. Lattuada, and A. Petri-Fink, *J. Mag. Magn. Mater.* **499**, 166176 (2020).
- [38] D. V. Berkov, N. L. Gorn, R. Schmitz, and D. Stock, *J. Phys.: Condens. Matter* **18**, S2595 (2006).
- [39] D. V. Berkov, L. Yu. Iskakova, and A. Yu. Zubarev, *Phys. Rev. E* **79**, 021407 (2009).
- [40] J. O. Sindt, P. J. Camp, S. S. Kantorovich, E. A. Elfimova, and A. O. Ivanov, *Phys. Rev. E* **93**, 063117 (2016).
- [41] A. O. Ivanov and P. J. Camp, *Phys. Rev. E* **98**, 050602(R) (2018).
- [42] T. M. Batrudinov, Yu. E. Nekhoroshkova, E. I. Paramonov, V. S. Zverev, E. A. Elfimova, A. O. Ivanov, and P. J. Camp, *Phys. Rev. E* **98**, 052602 (2018).
- [43] P. Ilg, *Phys. Rev. B* **95**, 214427 (2017).
- [44] P. Ilg and A. E. A. S. Evangelopoulos, *Phys. Rev. E* **97**, 032610 (2018).
- [45] P. Ilg, *Phys. Rev. E* **100**, 022608 (2019).
- [46] A. A. Kuznetsov, *Phys. Rev. B* **98**, 144418 (2018).
- [47] P. M. Déjardin, *J. Appl. Phys.* **110**, 113921 (2011).
- [48] A. O. Ivanov, V. S. Zverev, and S. S. Kantorovich, *Soft Matter* **12**, 3507 (2016).
- [49] T. M. Batrudinov, A. V. Ambarov, E. A. Elfimova, V. S. Zverev, and A. O. Ivanov, *J. Mag. Magn. Mater.* **431**, 180 (2017).
- [50] N. A. Usov, O. N. Serebryakova, and V. P. Tarasov, *Nanosc. Res. Lett.* **12**, 489 (2017).
- [51] A. Yu. Zubarev, *Phys. Rev. E* **98**, 032610 (2018).
- [52] A. Yu. Zubarev and L. Yu. Iskakova, *Physica A* **528**, 121500 (2019).
- [53] A. Y. Zubarev, *Phys. Rev. E* **99**, 062609 (2019).
- [54] A. F. Abu-Bakr and A. Zubarev, *Philos. Trans. Royal Soc. A* **377**, 20180216 (2019).
- [55] Yu. L. Raikher and V. V. Rusakov, *J. Mol. Liq.* **71**, 81 (1997).
- [56] W. Weitschies, R. Kötitz, T. Bunte, and L. Trahms, *Pharm. Pharmacol. Lett.* **7**, 5 (1997).
- [57] E. Romanus, M. Hückel, C. Groß, S. Prass, W. Weitschies, R. Bräuer, and P. Weber, *J. Magn. Magn. Mater.* **252**, 387 (2002).
- [58] Y. R. Chemla, H. L. Grossman, Y. Poon, R. McDermott, R. Stevens, M. D. Alper, and J. Clarke, *Proc. Natl. Acad. Sci. USA* **97**, 14268 (2000).
- [59] H. L. Grossman, W. R. Myers, V. J. Vreeland, R. Bruehl, M. D. Alper, C. R. Bertozzi, and J. Clarke, *Proc. Natl. Acad. Sci. USA* **101**, 129 (2004).
- [60] K. Enpuku and T. Minotani, *IEICE Trans. Electron.* **E84C**, 43 (2001).
- [61] F. Wiekhorst, U. Steinhoff, D. Eberbeck, and L. Trahms, *Pharm. Res.* **29**, 1189 (2012).
- [62] M.-D. Yang, C.-H. Ho, S. Ruta, R. Chantrell, K. Krycka, O. Hovorka, F.-R. Chen, P.-S. Lai, and C.-H. Lai, *Adv. Mater.* **30**, 1802444 (2018).
- [63] S. Chandrasekhar, *Rev. Mod. Phys.* **15**, 1 (1943).
- [64] LAMMPS Molecular Dynamics Simulator (2020), <http://lammmps.sandia.gov>.
- [65] S. Plimpton, *J. Comp. Phys.* **117**, 1 (1995).
- [66] J. J. Cerdà, V. Ballenegger, O. Lenz, and C. Holm, *J. Chem. Phys.* **129**, 234104 (2008).
- [67] J. D. Weeks, D. Chandler, and H. C. Andersen, *J. Chem. Phys.* **54**, 5237 (1971).
- [68] E. A. Elfimova, A. O. Ivanov, and P. J. Camp, *J. Chem. Phys.* **136**, 194502 (2012).
- [69] J. J. Weis and D. Levesque, *Phys. Rev. Lett.* **71**, 2729 (1993).
- [70] D. Levesque and J. J. Weis, *Phys. Rev. E* **49**, 5131 (1994).
- [71] P. J. Camp and G. N. Patey, *Phys. Rev. E* **62**, 5403 (2000).
- [72] P. I. C. Teixeira, J. M. Tavares, and M. M. Telo da Gama, *J. Phys.: Condens. Matter* **12**, R411 (2000).
- [73] A. O. Ivanov and S. S. Kantorovich, *Phys. Rev. E* **70**, 021401 (2004).